Nanoscale Res Lett (2010) 5:1377–1386
DOI 10.1007/s11671-010-9710-2

NANO REVIEW

Plasma-Assisted Synthesis of Carbon Nanotubes

San Hua Lim · Zhiqiang Luo · ZeXiang Shen · Jianyi Lin

Received: 31 May 2010 / Accepted: 19 July 2010 / Published online: 1 August 2010
© The Author(s) 2010. This article is published with open access at Springerlink.com

Abstract The application of plasma-enhanced chemical vapour deposition (PECVD) in the production and modification of carbon nanotubes (CNTs) will be reviewed. The challenges of PECVD methods to grow CNTs include low temperature synthesis, ion bombardment effects and directional growth of CNT within the plasma sheath. New strategies have been developed for low temperature synthesis of single-walled CNTs based the understanding of plasma chemistry and modelling. The modification of CNT surface properties and synthesis of CNT hybrid materials are possible with the utilization of plasma.

Keywords Plasma · Carbon · Nanotubes · Ion bombardment

Introduction

Carbon nanotubes (CNTs) are unique one-dimensional carbon materials which exist mainly as single-walled (SWNTs) and multi-walled carbon nanotubes (MWNTs). CNTs exhibit extraordinary properties such as high tensile strength, excellent electrical and thermal conductivities [1, 2]. A wide range of potential applications of CNTs have been envisioned in the field of computer logic and memory devices, interconnect via, nanosensors, field emitters, nanoactuators, polymer composites, catalyst supports and membranes [3–10]. Of particular interest is the electronic property of SWNTs, which are seamlessly rolled-up graphene sheets of carbon, behaving either as semiconductors or as metals depending on its diameters and chiralities [11]. Metallic SWNTs possess ballistic electron transport [12] and huge current carrying capacity while semiconducting SWNTs are interesting candidates for field-effect transistors [13]. The electronic properties of MWNTs depend on the features of each coaxial carbon shell, and electron conduction takes place within the basal planes (*a*-axis) of graphite [14]. As shown in Fig. 1a, the concentric graphite basal planes of MWNTs are parallel to the central axis ($\alpha = 0$). In the case $\alpha > 0$, the multi-walled carbon nanostructures are commonly called carbon nanofibres (CNFs) with their graphene layers arranged as stacked cones or plates, which exhibit a mixture of *a*-axis (basal plane) and *c*-axis (normal to basal plane) electron conduction [15–29]. Raman spectroscopy also distinguishes the structural differences between CNFs and MWNTs (see Fig. 1b). CNFs exhibit an additional shoulder at 1,612 cm^{-1} for the tangential graphitic G-band (typically located at $\sim$1,589 cm^{-1}), which is absent for ideal MWNTs [29]. The unique electronic conductions of one-dimensional carbon-based materials are useful for future microelectronics devices.

CNTs are commonly synthesized by laser ablation [30], arc discharge [31] and thermal chemical vapour deposition (TCVD) [32–34] methods. The choice of the synthesis technique is highly motivated by the field of applications. In the field of microelectronic application, controllable assembly and directional in situ synthesis of CNTs are very crucial steps to incorporate CNTs directly into the integrated circuit. Chemical vapour deposition methods offer the greatest potential for large-scale and commercially

S. H. Lim (✉) · Z. Luo · J. Lin
Institute of Chemical and Engineering Sciences, A*STAR, Singapore 627833, Singapore
e-mail: lim_san_hua@ices.a-star.edu.sg

Z. Luo · Z. Shen
Division of Physics and Applied Physics, School of Physical and Mathematical Sciences, Nanyang Technological University, Singapore 637616, Singapore

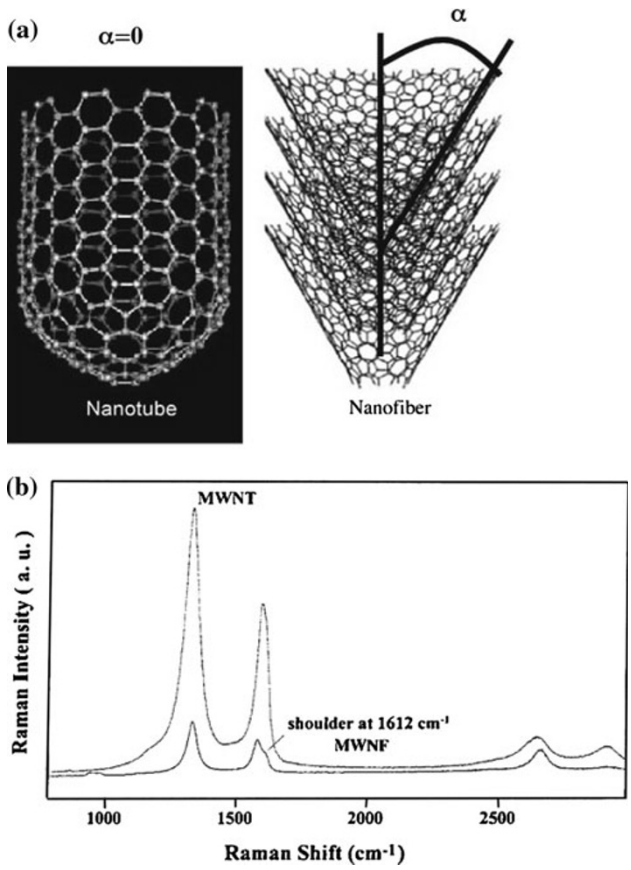

Fig. 1 **a** Structure of a carbon nanotube ($\alpha = 0$) and carbon nanofibre ($\alpha > 0$) produced by plasma-enhanced chemical vapour deposition. α is the angle between the central axis and the graphite basal planes. [Adapted from Ref 19] **b** Raman spectroscopy of MWNTs and CNFs. [Adapted from Ref 29]

viable synthesis of assembled CNTs. TCVD methods have also been traditionally used in integrated circuit manufacturing and therefore existing facilities are suitable for CNT growth.

However, the synthesis of CNTs using TCVD method requires undesirably high temperature, which damages the electronic chip. A milder synthesis condition is needed. Plasma-enhanced chemical vapour deposition (PECVD) method offers a solution to low temperature synthesis of CNTs. Likewise PECVD methods are also widely used in integrated circuit manufacturing for the growth of oxide and nitride thin films and its conversion for CNT growth will not be a major issue.

Early reports on PECVD methods required synthesis temperature as high as TCVD to grow CNTs (or CNFs). However, only PECVD methods synthesize free-standing, individual and vertically aligned (VA) CNTs. This unique feature distinguishes PECVD from TCVD and opens up the possibility of making nanodevices based on single strand CNT. Improvement in catalyst-support design, PECVD reactor setup, plasma conditions and synthesis parameters significantly help to lower the CNT synthesis temperatures to 400–500°C. Despite the advancement in PECVD studies of CNT growth, there are still many unresolved issues. For examples, the active carbon species responsible for the catalytic growth of nanotubes remain unclear. A credible low temperature (<400°C) synthesis of aligned CNT without compromising its crystallinity has not been reported. Self-termination of CNT growth due to catalyst poisoning is a common phenomenon and is it possible to avoid it and achieve uninterrupted growth in PECVD methods? The built-in electric field of a plasma sheath in a PECVD reactor has yet to be fully exploited to orient and align CNT growth. The PECVD methods also offer the opportunity to modify the properties of CNTs using plasma and create new hybrid materials. Thus, the intent of this review is to address these issues of CNT growth using PECVD methods. The review is organized as follows: "Challenges of PECVD Methods" discusses the challenges of PECVD methods with special focus on low temperature synthesis, ion bombardment effects and directional growth of CNT guided by electric and magnetic field. The modification of CNT using the plasma is presented in "Plasma Modification of CNTs". Concluding remarks are given in "Conclusion".

Challenges of PECVD Methods

Low Temperature Synthesis

Figure 2 showed a typical glow discharge encountered in a PECVD reactor. The plasma was generated by applying a direct current (DC) or radio frequency (<100–13.56 MHz) between two electrodes. The plasma is composed of electrons, charged ions and neutral molecules. The plasma remains electrically neutral as the ion density is balanced

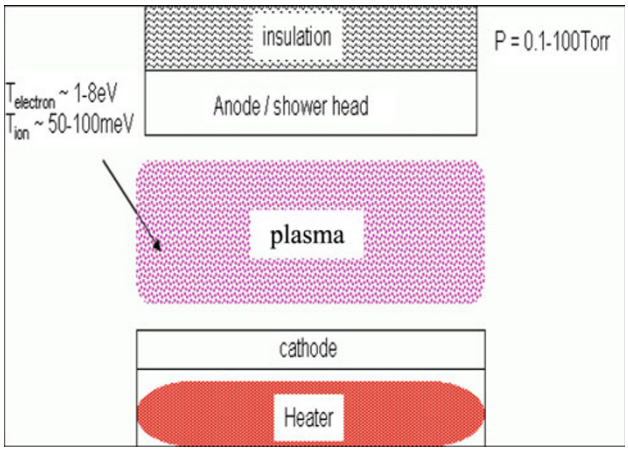

Fig. 2 A simplified diagram of a plasma-enhanced chemical vapour (PECVD) reactor

by the electron density. The electron density in the radio frequency generated plasma is typically $\sim 10^8$–10^9 cm^{-3} for a pressure range of 0.1–100 Torr. The electron temperatures are $\sim$1–8 eV, while the ion temperatures are lower at $\sim$50–100 meV. There is also a spontaneous but nonequilibrium conversion of neutral species into long-lived radicals. The plasma formed "sheaths", dark regions of very low electron density, with the electrodes. Sheath voltages were formed across these dark regions with the electrodes and the plasma forming the two plates. The substrate in a plasma sheath was bombarded with flux of ions and neutral species, whose kinetic energy varies from a few tens to several hundreds of eV [35, 36]. Electrons were confined within the plasma by the potential away from the sheath regions.

The plasma composition during PECVD growth of CNFs had been analysed using mass spectrometer and optical emission spectroscopy (OES) [26, 27]. Figure 3 showed the mass spectrum for neutral species detected during the synthesis of CNFs using C_2H_2 and NH_3 feedstocks in a dc PECVD reactor. The partial dissociation of C_2H_2 and NH_3 led to the formation of H_2, HCN, H_2O and N_2 species. The presence of excited neutral and ionized species was easily detected by measuring the optical emission intensity of the plasma. The OES of three different hydrocarbon gases diluted in NH_3 gases was displayed in Fig. 4. Emission from the hydrogen Balmer line

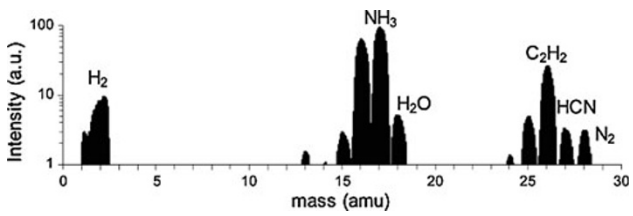

Fig. 3 Mass spectrum for neutral species [Adapted from Ref 26]

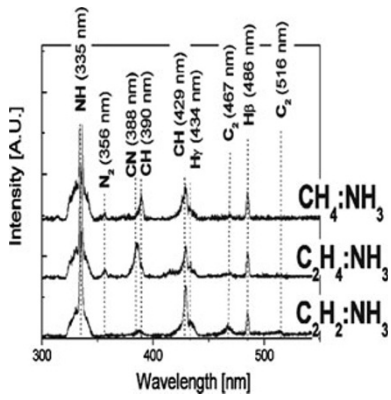

Fig. 4 Optical emission spectra of a 600 V dc discharge for hydrocarbons in ammonia dilution for nanofibre growth. [Adapted from Ref 27]

H_γ and H_β was identified at 434 and 486 nm, respectively. Emission bands from CH species corresponding to $A^2\Delta \rightarrow X^2\Pi$ (429 nm) transitions were also observed. The C_2 Swan bands located at 467 and 516 nm were only observable for C_2H_2 and C_2H_4 precursors. The results of MS and OES studies provided clues to the possible active species present in the plasma during the synthesis of CNFs but there is still a lack of information on the actual surface reaction of the catalysts.

The synthesis of carbon nanotubes or nanofibres requires temperature of 700–1,000°C using thermal chemical vapour deposition (TCVD) methods. This temperature requirement far exceeds the temperature limit of microelectronic, which is typically $\sim$400–500°C. Plasma-enhanced chemical vapour deposition (PECVD) method has been proposed as an alternative method to reduce the synthesis temperature. The plasmatic energy efficiently dissociates gas molecules at lower temperatures, and the synthesis of carbon nanotubes might occur at lower temperatures. The presence of a built-in electric field in a plasma sheath will align the growing CNTs along the field lines. Thus, PECVD methods favour low temperature synthesis of VA-CNTs.

Large-scale Monte Carlo simulations [37] of SWNT synthesis showed that PECVD methods were more suitable for low temperature synthesis and had two orders of magnitude higher growth rates than TCVD methods. In PECVD methods, the delivery and redistribution of carbon adatoms between the catalysts and the nanotubes' bases were more efficiently controlled than TCVD methods. Catalyst poisoning and amorphous carbon formation were prevented and resulted in uninterrupted ultralong plasma-assisted growth of SWNTs.

Table 1 summarized the synthesis of carbon nanotubes/nanofibres at low temperatures ($\leq$500°C) reported in literature. However, Teo et al. [20] revisited the results of low temperature (<400°C) growth of carbon nanofibres using a parallel plate dc PECVD reactor, and they showed that a high power plasma ($\sim$200 W) significantly induced heating of the substrates up to 700°C without the need of an external heater (see Fig. 5). A gas mixture of 54:200 sccm C_2H_2/NH_3 at a pressure of 12 mbar was used for the experiment. In other words, the substrate temperature might be different from the temperature of sample stage, which was heated by an external heater. Plasma-heating effect of the substrates casts doubts on the credibility of previously reported results of low temperature synthesis of CNTs/CNFs using high plasma power. However, plasma power of 200–300 W is commonly used in plasma-based process, and the substrate temperature has not been reported to increase significantly. The power density of the dc PECVD reactor, which is not stated by Teo et al. [20], might be responsible for the plasma-heating effect of the

Table 1 Low temperature (≤500°C) growth of carbon nanotubes/nanofibres using PECVD methods

	Temperature °C	Power W	Type of plasma[a]	Feedstock	Catalysts	Orientation	Reference
MWNTs/CNFs							
1	25	200	RF	CH_4:H_2 = 30:50 sccm	Ni powder (4–7 mm)	Random	38
2	25	200/400	DECR	C_2H_2/N_2 1 sccm	2 nm Ni film	Random	39
3	120	NA	DC	Ratio C_2H_2:NH_3 = 1:4	6 nm Ni film	Vertically aligned	27
4	200	1,000/60	ICP	$CH_4 + H_2$ = 30 sccm	33 nm Ni film	Vertically aligned	40
5	200	NA	DC	C_2H_2:NH_3 = 30:200 sccm	6 nm Ni film	Vertically aligned	17
6	250	20	DC	C_2H_2:NH_3 = 50:200 sccm	Ni/Co nanoparticles	Random	25
7	370	500	Microwave	CH_4/H_2	Fe-Si film	Vertically aligned	41
8	400	350	RF	CH_4:H_2 = 0.4:20 sccm	100 nm Ni film	Vertically aligned	42
9	450	180	RF	C_2H_2:NH_3 = 5:20 sccm	40–100 nm Ni films	Vertically aligned	43
10	500	1,000	ICP	Pure CH_4	30 nm Ni film	Vertically aligned	44
11	500	<20	DC	C_2H_2:NH_3 = 50:200 sccm	Ni/Fe/Co	Vertically aligned	24
SWNTs							
12	450	15	Remote RF	CH_4:Ar = 60:15 sccm	Fe/FeMo nanoparticles	Random	45/46
13	500	5	RF	C_2H_4:H_2 = 10:40	1 nm Fe film	Vertically aligned	47

[a] *RF* radio frequency, *DC* direct current, *ICP* inductively coupled plasma

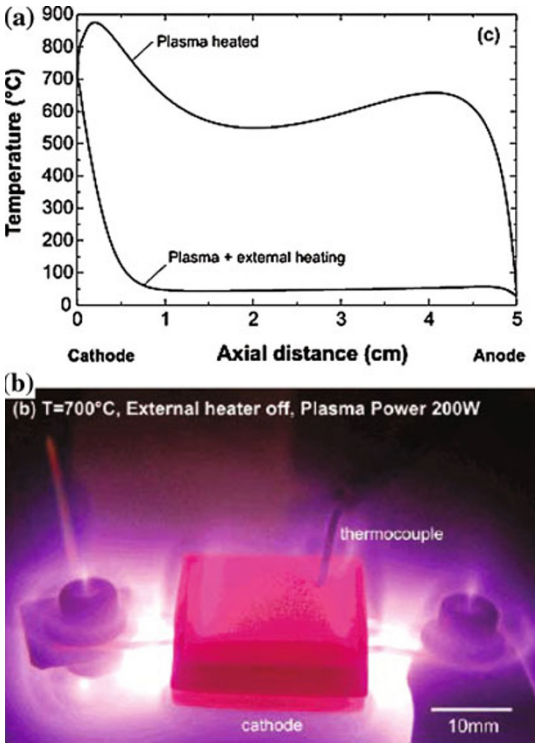

Fig. 5 **a** Measured and simulated cathode temperatures as a function of plasma power. The gas mixture simulated was 54:200 sccm C_2H_2/NH3 at 12 mbar. Cathode-to-anode temperature profiles for the cases of pure plasma heating vs plasma plus external heating. **b** Plasma heating of the cathode at 700°C, using 200 W of plasma power with the external heater off. The chamber was filled with a gas mixture of 54:200 sccm of C_2H_2/NH_3 at a pressure of 12 mbar. The thermocouple is mineral insulated with a stainless steel sheath and enters through the plasma (hot gas) zone before it is embedded in a 1–2 mm deep hole in the cathode. [Adapted from Ref 20]

substrate. Theoretical model [28] of carbon nanofibre growth in a PECVD method also indicated that a high flux of ion bombardment significantly increased the catalyst temperature at the tip of the nanofibre.

Would the growth mechanism of CNTs depend on temperature? The growth of CNTs synthesized using high temperature TCVD methods had been proposed to be a vapour-liquid-solid mechanism [48]. The catalyst was in a liquid drop state and carbon species from the chemical vapour dissolved into it. Carbon nanotubes were precipitated from the supersaturated eutectic liquid. The activated energy for TCVD (≤700°C) was reported to be ~1.2–1.8 eV [49, 50]. Clearly, this proposed growth mechanism of CNTs was not suitable for low temperature growth (<120°C), whereby the catalysts might remain as solids at such low temperatures. Low activation energy of ~0.2–0.4 eV was reported for low-temperature plasma-assisted growth of CNTs [27, 51], which was similar to the activation energy of surface diffusion of carbon atoms on polycrystalline Ni (0.3 eV) [52]. Hoffman et al. [51] suggested that the rate-limiting step for low temperature plasma-assisted growth of CNTs was the carbon diffusion on the catalyst surface.

Ion Bombardment Effects on SWNT Growth

Early attempts to use PECVD process to synthesize carbon nanotube yielded mostly VA-MWNTs and CNFs. In order to synthesize SWNTs, it required the use of special plasma configuration such as remote plasma or point arc discharge, whereby the substrates were minimally exposed to the

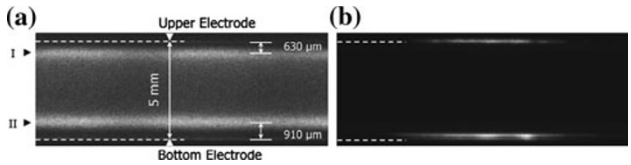

Fig. 6 Emission distribution of CH (432 nm) in different operation regimes of APRFD. Emission intensity in the α-mode is 10 times greater than that of α-mode regime: **a** α-mode (60 W), **b** α-mode (100 W). [Adapted from ref 54]

plasma sheath. Goheir et al. [52, 53] showed that the exposure of substrates to the plasma sheath inevitably resulted in the transition of SWNTs to MWNTs, which was attributed to ion bombardment effects. In the plasma sheath, there was a high density of plasma ion flux ($n_{ion} \sim 10^{10}$ cm^3) which bombarded SWNTs at sufficiently high energy of ~100 eV and caused C–C bond breakage. The presence of plasma radicals such as NH_x and H further chemically etched the surface of the carbon nanotubes. The growth mechanism of SWNT in a PECVD process determines the resistibility of the carbon nanotubes towards ion-etching effects. In the tip-growth mechanism, the catalyst was at the tip of the vertically growing SWNT, offered protection to walls of the nanotube from the ion-etching effects. On the other hand, in base-growth mechanism, the catalyst was adhered to the substrate, and the vertically growing SWNTs had uncapped tips, which were easily destroyed by the impinging ions. Consequently, a transition from SWNTs to MWNTs in a PECVD process was observed since the multiple layers of carbon were more resistant towards ion etching.

As shown in Fig. 6, the operation mode of plasma transited from a so-called α-mode (60 W) to γ-mode (100 W) as the input power was increased from 60 to 100 W in an atmospheric pressure radio frequency discharge (APRFD) reactor [54, 55]. In the α-mode, emission layers were due to the spectra of CH at 432 nm and created near momentary cathode (I and II). Plasma sheaths of 630–910 μm thickness were formed between momentary cathode layers and electrodes. The potential dropped drastically from the momentary cathode layers (I and II) towards the electrodes. As the input power was increased, which favoured the transition to a γ-mode, the electric field strength in the plasma sheath also increased and caused more energetic ion bombardment. When the ion hit the electrodes, secondary electrons were generated and accelerated into the plasma sheath by the electric field, which caused more intense ionization in the vicinity of electrodes. The schematic diagram of γ-mode plasma is presented in Fig. 7. Thus, the presence of very intense plasma spots was observed in the γ-mode which induced plasma-heating effects of the catalysts and damaged CNTs. The mode of the plasma had great impact on the synthesis of SWNTs

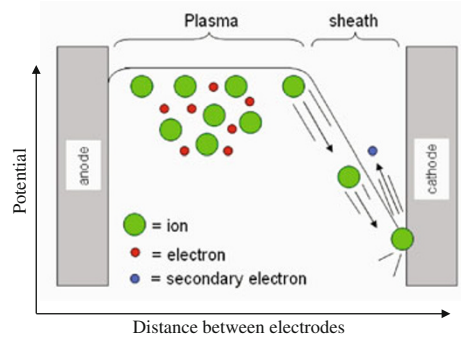

Fig. 7 A schematic representation showing the variation of potential between two parallel plate electrodes

and undesirable ion bombardment of substrate should be avoided in order to growth SWNTs.

On the other hands, Luo et al. [47] synthesized high quality VA-SWNTs in a plasma sheath of a capacitively coupled rf PECVD by optimizing two controllable experimental parameters, namely plasma input power (sheath voltage, V) and gas pressure, and thereby reducing ion bombardment effects. On the basis of a simplified ion space-charge-limited model [56], the plasma ion flux (n_{ion}) and ion energy (E_{ion}) were qualitatively related to gas pressure (P) and sheath voltage (V) as follow:

$$E_{ion} \propto V^{4/5} P^{-1/2} \quad (1)$$

$$n_{ion} \propto V P^{3/4} \quad (2)$$

When the gas pressure (P) was fixed, the increment of plasma input power significantly increased the ion flux impinging SWNTs, while the ion energy was moderately increased. On the other hand, for a fixed plasma input power, the plasma sheath varied with pressure as $V \propto P^{1/2}$. The plasma ion flux and energy can be rewritten as follow: $E_{ion} \propto P^{-1/10}$ and $n_{ion} \propto P^{5/4}$, which indicated that the ion-etching effects were dominated by the ion flux. The reduction of incoming ion flux was essential to the synthesis of high quality SWNTs in a plasma sheath. On the basis of Eqs. 1 and 2, there is always ion bombardment in a plasma sheath during SWNT growth but the degree of ion bombardment is minimized by tuning the sheath voltage and reactor pressure in order to achieve SWNT growth.

Luo et al. [47] showed that the resistibility of VA-SWNTs against ion etching was dependent on the synthesis temperature. At temperatures ≥600°C, the ion-etching effects did not damage the VA-SWNTs significantly. When the temperatures were lowered to ≤500°C, the growth rate of SWNT was reduced, and ion-etching effects became significant. The conversion of SWNTs into MWCNTs by low energy hydrogen bombardment is still possible at low temperature synthesis, particularly when the ion-etching rate is faster than the CNT growth rate.

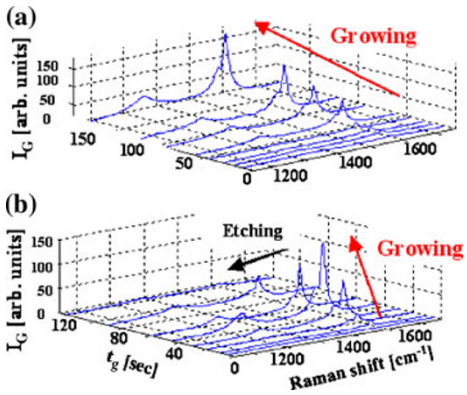

Fig. 8 Raman spectra of SWNTs as a function of t_g. **a** $P_{rf} = 40$ W and **b** $P_{rf} = 100$ W, respectively. [Adapted from ref 57]

Kato et al. [57] studied the kinetics of reactive ion etching on the synthesis of SWNTs in a parameter-controlled PECVD reactor. Figure 8 showed the time evolution of the graphitization of SWNTs synthesis due to reactive ion-etching effects. The growth kinetics of SWNTs was monitored using Raman spectroscopy whereby the degree of graphitization of SWNTs was assumed to be related to its tangential mode (I_G). For weak and negligible ion etching, the growth kinetics of SWNTs in a PECVD method at 750°C was very similar to a thermal CVD process, which can be expressed as follow:

$$I_G = I_o\left[1 - \exp\left[-\left(\frac{t_g - \Delta_t}{\tau_{gro}}\right)\right]\right] \quad (3)$$

where I_o, Δt and τ_{gro} denote saturated tangential modes of SWNTs, incubation time, and relaxation time of the growth, respectively. To account for significant etching effect, Kato et al. proposed a new growth equation for the growth kinetics of SWNTs:

$$I_G = I_o \exp\left[\frac{-t_g}{\tau_{etc}}\right]\left\{1 - \exp\left[\frac{-(t_g - \Delta t)}{\tau_{gro}}\right]\right\} \quad (4)$$

where τ_{etc} denotes relaxation time of the etching. The modified growth kinetics model of SWNTs, which included the ion-etching effects, agreed well with experimental results. The modified growth kinetics model of SWNTs predicted that the presence of high radical densities in hydrocarbon plasma, particularly H densities, also contributed to the etching effects.

Zhang and Qi et al. [58] showed that a methane plasma selectively etched metallic SWNTs while semiconducting SWNTs remained unmodified. Metallic SWNTs were irreversibly etched into hydrocarbon gas species as a result of ion bombardment of H and CH_3 ion species present in methane plasma. Small-diameter SWNTs were preferentially etched over larger ones because of the higher radius curvature and strain in the C-C bonding. This finding had great implication for controlling the electronic properties of SWNTs synthesized in a PECVD process. Theoretical studies [1, 2] had predicted that ~1/3 of as-synthesized SWNTs was metallic, and the remaining ~2/3 nanotubes were semiconducting. In other words, the SWNTs synthesized in PECVD methods composed mainly of semiconducting tubes. Li and Qu et al. [59, 60] also demonstrated the preferential synthesis of semiconducting SWNTs in a PECVD, whereby the metallic SWNTs will inherently destroyed during the synthesis steps.

Several strategies had been developed to minimize the effects of reactive ion etching which were inherent in PECVD processes. Nozaki et al. [54, 55] had developed an atmospheric pressure radio frequency PECVD to synthesize VA-SWNTs. The high collision frequency of the molecules at atmospheric pressure significantly reduced the ion etching of the SWNTs. In a remote downstream PECVD process [45, 46], high density plasma was generated at a distance from the SWNT substrates such that the plasma sheath was not close to the substrates and reduced the ion-etching effects. Kato et al. [61] diffused the spatial distribution of plasma by forming a small hole (diameter 10 mm) in the centre of the bottom electrode while the substrate placed below it. This diffusion PECVD method reduced ion bombardment and promoted the growth of free-standing individual SWNTs.

Controlling Alignment of CNTs

In a PECVD process, the free-standing CNTs were aligned along the direction of the electrical field in the plasma sheath. Experimental studies showed that the CNT alignment was dependent on the catalytic nanoparticles in the tips of the tubes. Alignment of free-standing CNTs in a field was observed for tip-growth model but not base-growth model. The high polarizability of CNTs in an electric field also assisted its directional growth. However, the vertical alignment of dense CNT forests, which were synthesized in base-growth model, was also observed in a PECVD process. In this case, the alignment of CNT forests was due to the collective van dar Waals interaction among the tubes (crowding effects).

Merkulov et al. [62] made a similar observation for the alignment of CNFs synthesized by PECVD. The locations of the catalyst nanoparticles for aligned and nonaligned CNFs were observed to be at the tips and bases of CNFs, respectively. The nonalignment of CNFs was due to the bending of the nanofibres during synthesis. Merkulov et al. [62] proposed that the alignment of CNFs was due to a feedback mechanism associated with a tensile-compressive stress generated at the catalyst-CNF interface (see Fig. 9). Neither ion bombardment nor electrostatic attraction played an important role for the bending of CNFs. When

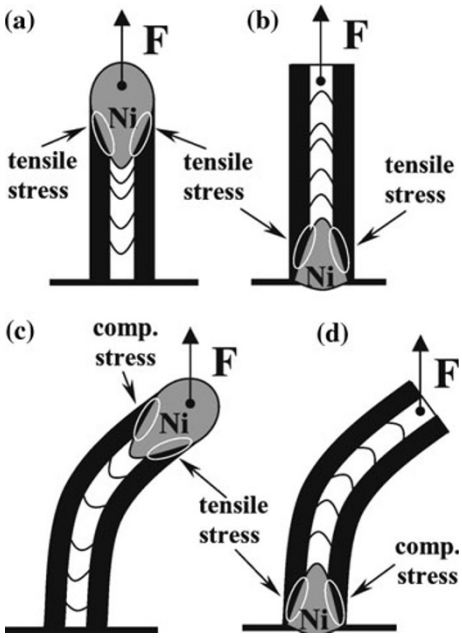

Fig. 9 Bending of carbon nanofibres due to spatial fluctuations in carbon precipitation at the Ni catalyst/nanofibre interface. [Adapted from ref 62]

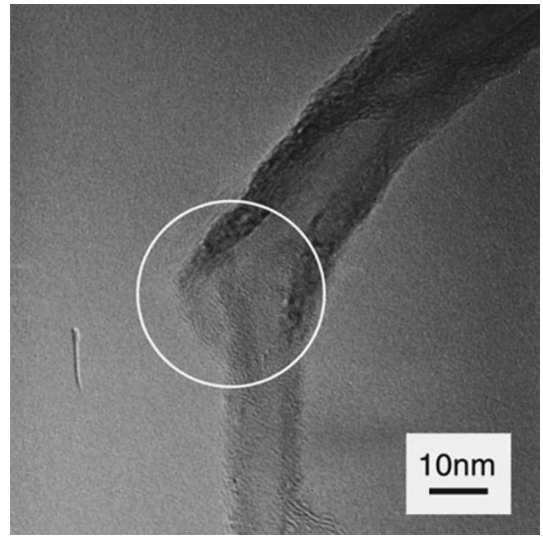

Fig. 10 Transmission electron micrograph showing the bending of carbon nanotube wall during growth when the magnetic field was changed. [Adapted from ref 63]

the axes of CNFs were growing perpendicularly to the substrates along the direction of the electric field, a uniform tensile stress occurred across the catalyst-CNF interface (see Fig. 9a, b), and the CNFs would be vertically aligned. However, as shown in Fig. 9c, d, CNFs would bend if there was a fluctuation in the carbon precipitation at the catalyst-CNF interface. For tip-growth model, the catalyst-CNF interface experienced a negative feedback which equalized the fluctuation of the carbon precipitation and re-aligned the CNFs for vertical growth. When the catalyst-CNF interface was attached to the substrate (base-growth model), the tensile stress resulted in greater precipitation of carbon than the compressive stress and caused the CNFs to bend significantly. An unstable positive feedback occurred and resulted in nonaligned CNFs.

When ferromagnetic iron nanocatalysts were at the tips of CNTs, the growth direction of CNTs was controllable by applying an external magnetic field in a PECVD process. In this case, an external magnetic field is applied for the directional growth of CNTs instead of the built-in electric field within the plasma sheath. As shown in Fig. 10, Ohmae et al. [63] synthesized bend CNTs by varying the magnetic field direction (10 mT) during CNT growth. A mixture of H_2/CH_4 with flow rates of 100 and 10 sccm was used to synthesize CNT at 700°C and pressure of 2.7×10^3 Pa. Hook-, arch-, and ladder-shaped CNT bundles were observed when the direction of magnetic field was repeatedly changed during the PECVD process. Ohmae et al. [63] suggested that the iron nanoparticles were ellipsoidal in shape, and the major axes were along the growth direction of CNTs. The iron nanoparticles followed the direction of magnetic field during growth and therefore the field controlled the alignment of CNTs. The self-bias of the PECVD, the electric potential between the plasma and substrate, was estimated to be-10 eV. A high electric field (10^3–10^4 V/m) was generated by this self-bias and the application of an external electric field to control the directional growth of CNT will be less effective than magnetic field.

The conductivity of substrates has a strong effect on the alignment of the nanotubes within the plasma sheath. When a conductive substrate was used to synthesize CNTs in a PECVD process, the electric field lines of the plasma sheath were always perpendicular to the substrate. On the other hand, when an insulating surface was deposited on top of the conducting substrate, a phenomenon known as plasma-induced surface charging occurred in the presence of an electric field of plasma sheath. The insulating surface accumulated net negative charges quickly and repelled the electron flux. In a steady-state plasma, the potential of the insulating surface (V_f) coupled to the plasma potential (V_P) via the sheath: $V_f = Vp - V_{sh,}$ where V_P and V_{sh} is the potential of the plasma and plasma sheath, respectively.

Law et al. [64] made use of this plasma-induced surface charging phenomenon to redirect electric field of the plasma sheath to be horizontally across two adjacent electrodes and achieve horizontal growth of CNTs. As shown in Fig. 11a "floating" electrode, which was separated from the substrate by an insulator, developed a floating potential V_{fe} with respect to the plasma potential. The potential of substrate (V_{fsub}) was the plasma potential at the wafer edges. Consequently, an electric field was

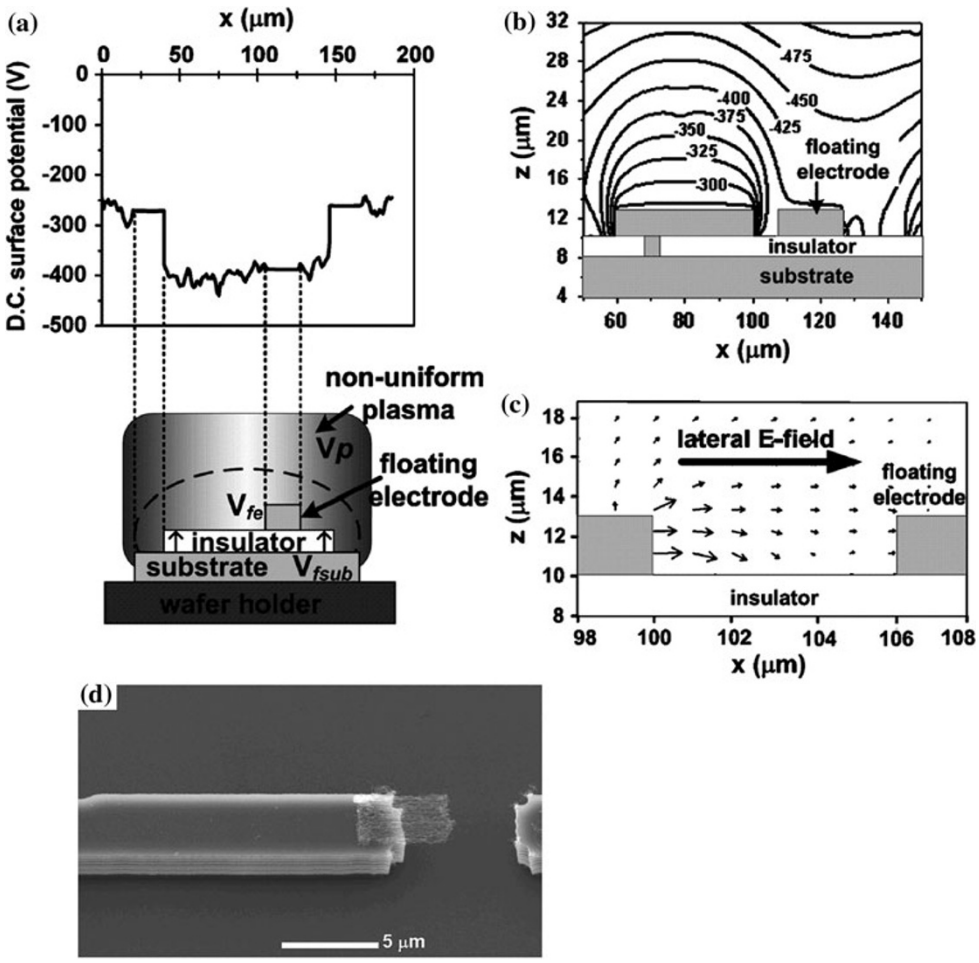

Fig. 11 OOPIC PRO simulation showing (**a**) difference in surface potential between the substrate and the isolated electrode in a plasma, (**b**) equipotential lines due to charging encountered by the geometry, and (**c**) electric field vectors in the vicinity of the gap between the electrode pair in **b**. **d** Horizontally directed growth of MWNTs from the short/float electrode pair. [Adapted from ref 64]

developed across the insulator due to the potential difference of V_{fe} and V_{fsub} (see Fig. 11). Chai et al. [65] had also applied the same principle and achieved horizontal growth of CNTs in a modified plasma sheath.

Similarly inclined CNTs were synthesized in the plasma sheath by orienting the electric field lines with respect to the substrate surface [66, 67]. Lin et al. [67] synthesized inclined CNTs by placing a tilted substrate in a plasma sheath which had electric field lines travelling vertically from the plasma to the sample stage. The corners of microstructures in the proximity of the substrates would also distort the electric field and yield inclined CNTs. The ability to control the inclination of CNT with respect to the substrate surface had important technical implications. For examples, inclined CNTs might be used as AFM probe tips and microfluidic channel as a valve or filter.

Plasma Modification of CNTs

We had successfully encapsulated linear carbon chains within VA-SWNTs (C_n@SWNTs) using a low plasma power in a PECVD process. Figure 12 shows the high-resolution transmission electron microscopy image of linear carbon chains encapsulated within SWNTs. Encapsulated linear carbon chains within carbon nanotubes has a unique characteristic Raman signal located $\sim$1,850 cm^{-1} (L-bands). Our Raman studies indicate the presence of L-bands and confirmed the existence of linear carbon within the SWNT samples. Theoretical studies of carbon plasma [68] predicted that using low temperature and power density plasma will yield a graphite-like flat sp^2 network while some remaining *sp* chains play the role of defects connecting neighbouring graphite-like fragments. The scenario for the growth of VA-C_n@SWNTs might be due to the employment of very low plasma power ($\sim$5 W). We had used a K-type thermocouple to measure that temperature of the plasma, and there was no plasma-heating effect at 5 W so that the formation of *sp* linear carbon chains was generated in the carbon plasma. Thus, a fraction of the *sp* linear carbon chains were encapsulated within SWNTs as the nanotubes were catalytically synthesized.

Other nano-sized graphitic materials were also attached carbon nanotubes in a PECVD process. Nano-sized

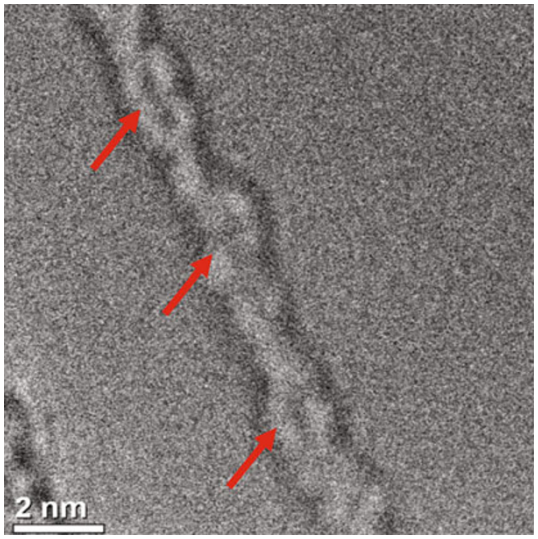

Fig. 12 High resolution transmission electron micrograph of linear carbon chains (indicated by red arrows) encapsulated within a single-walled carbon nanotubes

graphite flakes were attached on the exterior of VA-CNTs for prolonged synthesis duration or the absence of etchant dilutant gases such as H_2 and NH_3 in PECVD processes [69, 70]. Malesevic et al. [70] also demonstrated a combined growth of carbon nanotubes and carbon nanowalls in a PECVD process. It was proposed that the excess carbon radicals over saturated the catalysts and terminated the CNT growth. The remaining carbon species were deposited in the form of graphitic sheets in the vicinity of the CNT tips.

Abdi et al. [71] synthesized branched carbon nanotubes, a PECVD process. A 5 nm layer of nickel catalysts were deposited on a silicon wafer. After the synthesis of VA-CNTs, a conformal layer of TiO_2 was coated on the exterior of the VA-CNTs. Hydrogen plasma was used to etch the TiO_2 coated VA-CNTs' tips and exposed the embedded Ni catalysts, which were subsequently used to grow branched CNTs. Branched CNTs were expected to have improved field emission and gas detection properties.

Surface functionalization of the CNTs had been achieved using PECVD methods. Various etchants such as Ar, H_2, O_2 and fluoride gases had been used to modify the surface properties of CNTs [72, 73]. For examples, under optimal conditions, treatment of CNTs with Ar and H_2 plasma improved its field emission properties. Li et al. [74] also showed that the wettability of as-synthesized CNTs could be carefully tuned from hydrophobic to hydrophilic using O_2 plasma. X-ray photoelectron spectroscopy revealed that OH–C=O groups, which increased the hydrophilicity of the plasma-treated CNTs, were formed at the open tips.

Conclusion

This article reviewed the synthesis of carbon nanotubes using PECVD methods. The utilization of plasma helped to lower the synthesis temperature of CNTs but excessive ion bombardment hindered SWNT growth. The growth of SWNTs was achieved when ion bombardment was minimized. The rate-determining step for low temperature PECVD growth of CNTs was suggested to be surface carbon diffusion. Therefore, future work should focus on the preparation, characterization and modelling of catalysts suitable for surface diffusion mechanism. Lab-scale fabrication of horizontally aligned CNTs with in the plasma sheath was demonstrated. However, current strategy of aligning CNTs horizontally within the plasma sheath might not be practical for actual device manufacturing. The application of an external electric field to synthesize horizontally aligned CNTs might still be required for large area synthesis. When compared to wet chemical treatment, plasma treatment of VA-CNT thin films was a useful 'dry' method to modify its surface properties without destroying the thin film integrity.

Open Access This article is distributed under the terms of the Creative Commons Attribution Noncommercial License which permits any noncommercial use, distribution, and reproduction in any medium, provided the original author(s) and source are credited.

References

1. F. Harris, *Carbon Nanotubes and Related Structures* (Cambridge Univ. Press, Cambridge, UK, 1999)
2. M.S. Dresselhaus, G. Dresselhaus, P. Avouris (eds.), *Carbon Nanotubes* (Springer, Berlin, Germany, 2001)
3. T. Rueckes, K. Kim, E. Joselevich, G.Y. Tseng, C. Cheung, C.M. Lieber, Science **289**, 94 (2000)
4. A.P. Graham, G.S. Duesberg, R. Seidel, M. Liebau, E. Unger, F. Kreup, W. Honlein, Diamond Relat. Mater. **1296**, 13 (2004)
5. Z.L. Li, P. Dharap, S. Nagarajaiah, E.V. Barrera, J.D. Kim, Adv. Mater. **16**, 640 (2004)
6. W.I. Milne, K.B.K. Teo et al., J. Mater. Chem. **14**, 933 (2004)
7. A.M. Fennimore, T.D. Yuzvinsky, W.Q. Han, M.S. Fuhrer, J. Cumings, A. Zettl, Nature **424**, 408 (2003)
8. J. Suhr, N. Koratkar, P. Keblinski, P. Ajayan, Nat. Mater. **4**, 134 (2005)
9. X. Wang, W. Li, Z. Chen, M. Waje, Y. Yan, J. Power Sources **158**, 154 (2006)
10. B.J. Hindus, N. Chopra, T. Randell, R. Andrews, V. Gavalas, L.G. Bachas, Science **303**, 62 (2004)
11. T.W. Odom, J. Huang, P. Kim, C.M. Lieber, Science **391**, 62 (1998)
12. C.T. White, T.N. Todorov, Nature **393**, 240 (1998)
13. A. Javey, H. Kim et al., Nat. Mater. **1**, 241 (2002)
14. N. Nihei, D. Kondo, A. Kawabata, S. Sato, H. Shioya, M. Sakaue, T. Iwai, M. Ohfuti, Y. Awano, Proc. IITC. (San Francisco, CA, Jun. 6–8, 2005), p. 234
15. K.B.K. Teo et al., Appl. Phys. Lett. **79**, 1534 (2001)
16. M. Chhowalla et al., J. Appl. Phys. **90**, 5308 (2001)

17. S. Hoffmann, C. Ducati, B. Kleinsorge, J. Robertson, Appl. Phys. Lett. **83**, 4661 (2003)
18. B.A. Cruden, A.M. Cassell, Q. Ye, M. Meyyappan, J. Appl. Phys. **94**, 4070 (2003)
19. Q. Ngo et al., IEEE Trans. Nanotechnol. **6**, 688 (2007)
20. K.B.K. Teo et al., Nano. Lett. **4**, 921 (2004)
21. C. Ducati et al., J. Appl. Phys. **95**, 6387 (2004)
22. A.M. Cassell et al., Nanotechnology **15**, 9 (2004)
23. S. Hofmann et al., J. Appl. Phys. **98**, 034308 (2005)
24. S. Hofmann et al., Appl. Phys. A **81**, 1559 (2005)
25. M. Cantoro et al., Diamond Relat. Mater. **14**, 733 (2005)
26. M.S. Bell, Pure Appl. Chem. **78**, 1117 (2006)
27. S. Hofmann et al., Diamond Relat. Meter. **13**, 1171 (2004)
28. I. Denysenko, K. Ostrikov, J. Phys. D Appl. Phys. **42**, 015208 (2009)
29. L. Delzeit et al., J. Appl. Phys. **91**, 6027 (2002)
30. C.T. Kingston, B. Simard, J. Nanosci. Nanotechnol. **6**, 1225 (2006)
31. M. Keidar et al., Appl. Phys. Lett. **92**, 043129 (2008)
32. M. Meyyappan, L. Delzeit, A. Cassell, D. Hash, Plasma Sources Sci. Technol. **12**, 205 (2003)
33. C.H. See, A.T. Harris, Ind. Eng. Chem. Res. **46**, 997 (2007)
34. A.V. Melechko et al., J. Appl. Phys. **97**, 041301 (2005)
35. Lieberman MA, Lichtenberg AJ, Principles of Plasma 2005 Discharge and Materials Processing 2nd edn. (Wiley, New York)
36. Y.P. Raier, M.N. Shneider, N.A. Yatsenko, *Radio-frequency Capacitive Discharges* (CRC Press, Boca Raton, FL, 1995)
37. E. Tam, K. Ostrikov, Appl. Phys. Lett. **93**, 261504 (2008)
38. B.O. Boskovic et al., Nat. Mater. **1**, 165 (2003)
39. T.M. Minea et al., Appl. Phys. Lett. **85**, 1244 (2004)
40. K.Y. Lee et al., Jpn. J. Appl. Phys. **42**, L804 (2003)
41. J.M. Ting, K.H. Liao, Chem. Phys. Lett. **396**, 469 (2004)
42. Y. Shiratori et al., Appl. Phys. Lett. **82**, 2485 (2003)
43. H.S. Kang et al., Chem. Phys. Lett. **349**, 196 (2001)
44. S. Honda et al., Jpn. J. Appl. Phys. **42**, L441 (2003)
45. E.J. Bae et al., Chem. Mater. **17**, 5141 (2005)
46. Y.S. Min et al., J. Am. Chem. Soc. **127**, 12498 (2005)
47. Z. Luo et al., Nanotechnology **19**, 255607 (2008)
48. J. Gavillet et al., Phys. Rev. Lett. **87**, 275504 (2001)
49. D.B. Geohegan et al., Appl. Phys. Lett. **83**, 1851 (2003)
50. Y.T. Lee et al., J. Phys. Chem. B **106**, 7614 (2002)
51. J.F. Mojica, L.L. Levenson, Surf. Sci. **59**, 447 (1976)
52. A. Gohier et al., J. Appl. Phys. **101**, 054317 (2007)
53. A. Gohier et al., Chem. Phys. Lett. **421**, 242 (2006)
54. T. Nozaki et al., Carbon **45**, 364 (2007)
55. T. Nozaki, K. Okazaki, Plasma Process. Polym. **5**, 300 (2008)
56. A. Godyak et al., IEEE Trans. Plasma Sci. **19**, 600 (1991)
57. T. Kato, R. Hatakeyama, Appl. Phys. Lett. **92**, 031502 (2008)
58. G. Zhang, P. Qi et al., Science **314**, 974 (2006)
59. Y. Li et al., Nano Lett. **4**, 317 (2004)
60. L. Qu, F. Du, L. Dai, Nano Lett. **8**, 2682 (2008)
61. T. Kato et al., Nanotechnology **17**, 2223 (2006)
62. V.I. Merkulov et al., Appl. Phys. Lett. **79**, 2970 (2001)
63. N. Ohmae, Carbon **46**, 544 (2008)
64. J.B.K. Law, C.K. Koo, J.T.L. Thong, Appl. Phys. Lett. **91**, 243108 (2007)
65. Y. Chai, Z. Xiao, P.C.H. Chan, Appl. Phys. Lett. **94**, 043116 (2009)
66. K. Gjerde et al., Carbon **44**, 3030 (2006)
67. C.C. Lin et al., Nanotechnology **15**, 176 (2004)
68. Y. Yamaguchi et al., Phys. Rev. B **76**, 134119 (2007)
69. R.E. Morjan et al., Chem. Phys. Lett. **383**, 385 (2004)
70. A. Malesevic et al., Carbon **45**, 2932 (2007)
71. Y. Abdi et al., Carbon **46**, 1611 (2008)
72. S.J. Kyung et al., Carbon **46**, 1316 (2008)
73. Z. Hou et al., Carbon **46**, 405 (2008)
74. P. Li et al., J. Phys. Chem. B **111**, 1672 (2007)